

Forearc Deformation and Great Subduction Earthquakes: Implications for Cascadia Offshore Earthquake Potential

Robert McCaffrey* and Chris Goldfinger

The maximum size of thrust earthquakes at the world's subduction zones appears to be limited by anelastic deformation of the overriding plate. Anelastic strain in weak forearcs and roughness of the plate interface produced by faults cutting the forearc may limit the size of thrust earthquakes by inhibiting the buildup of elastic strain energy or slip propagation or both. Recently discovered active strike-slip faults in the submarine forearc of the Cascadia subduction zone show that the upper plate there deforms rapidly in response to arc-parallel shear. Thus, Cascadia, as a result of its weak, deforming upper plate, may be the type of subduction zone at which great (moment magnitude ≈ 9) thrust earthquakes do not occur.

The largest known earthquakes result from the thrusting of oceanic lithosphere beneath the forearc of the overriding plate at subduction zones. Some subduction zones have produced earthquakes in this century with moment magnitudes M_w (1) in excess of 9, whereas others have had events of only $M_w \approx 8$ or less. At the Cascadia subduction zone (CSZ) off the coast of Oregon and Washington, no great thrust earthquakes have occurred in historical times and it is debated whether one can occur. A recently discovered feature of the CSZ relevant to this debate is upper-plate deformation evident in several faults that cut the forearc at a high angle to the trench (2, 3). To understand the significance of such faults for earthquake potential, we examined subduction zones around the world and found a trend that suggests that deformation within the leading edge of the overriding plate limits the size of thrust earthquakes. These observations and a geologic estimate of the deformation rate within the upper plate at Cascadia suggest that the CSZ is more like the type of subduction zone that does not produce thrust earthquakes significantly larger than $M_w \approx 8$ than like the type that does. We estimate that the offshore strike-slip faults within the forearc will produce earthquakes smaller than about $M_w \approx 7.5$ and pose a smaller hazard to onshore areas than $M_w \approx 8$ or greater subduction events. We do not assess the seismic hazards due to onshore crustal faults or those due to earthquakes in the subducted lithosphere beneath Oregon and Washington (4).

Kanamori (5) proposed that the observed

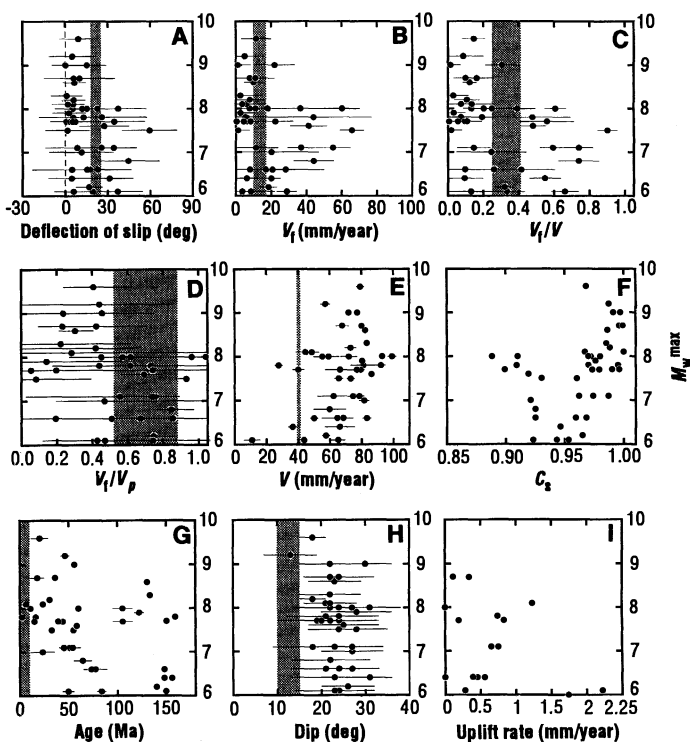
variation in seismic energy release among subduction zones is due to coupling between the plates: strong coupling produces large earthquakes, whereas weakly coupled zones slip aseismically. Coupling was thought to be enhanced by fast subduction rate, low dip and young age of the subducting plate, and thick trench sediments (6). Using such reasoning, it was proposed that the CSZ is of the type that is characterized by great thrust earthquakes, largely because the subducting lithosphere there is very young, the dip is

gentle, and the trench sediments are thick (7).

From a global examination of subduction zones, we find that forearc deformation rates limit the maximum sizes of thrust earthquakes (Fig. 1). Anelastic, arc-parallel motion of the leading edge of the upper plate relative to the backarc region deflects the slip directions of subduction-zone thrust earthquakes away from expected plate-convergence directions (8). The magnitudes of these slip deviations provide the arc-parallel rate of the forearc motion relative to the upper plate. Deviations of slip are relatively small in regions where $M_w > 8$ subduction thrust earthquakes have occurred in this century (9) (Fig. 1A), suggesting that great earthquakes tend to occur in subduction zones characterized by undeforming forearcs. Two possible explanations are that thrust faults beneath rapidly deforming forearcs are more heterogeneous (10) than those beneath undeforming forearcs or that deforming forearcs respond to stress by anelastic (11), rather than elastic, strain.

The size of the largest earthquake observed at subduction zones decreases both with the rate of forearc deformation (Fig. 1B) and with this rate normalized by the full plate convergence rate (Fig. 1C). Forearcs that move along the arc at rates of more than half the arc-parallel component of plate mo-

Fig. 1. Relations of various properties of subduction zone segments to the largest earthquake (maximum moment magnitude, M_w^{\max}) to occur in that segment during this century. Shading shows the estimated range for Cascadia. The world's trenches are divided into segments 500 to 1000 km long, and properties are averaged in each segment. Each dot represents one of these segments, and error bars are 1 SD. The procedure is described in (14). (A) Deflection of the average slip direction of thrust earthquakes away from the expected plate convergence direction; (B) V_f , the rate of forearc arc-parallel motion relative to the upper plate inferred from slip deflections; (C) arc-parallel forearc motion normalized by plate convergence rate V ; (D) arc-parallel forearc motion normalized by the arc-parallel component of relative plate motion V_p ; (E) plate convergence rate; (F) seismic consistency C_s (13); (G) the age of the subducting lithosphere (30); (H) dip angle of the top of the subducting slab inferred from earthquakes; and (I) uplift rate of forearcs derived from the height of 125,000-year-old coral terraces at several subduction zones (27).



R. McCaffrey, Department of Earth and Environmental Sciences, Rensselaer Polytechnic Institute, Troy, NY 12180, USA.

C. Goldfinger, College of Oceanic and Atmospheric Sciences, Oregon State University, Corvallis, OR 97331, USA.

*To whom correspondence should be addressed.

tion do not have earthquakes greater than about $M_w = 8$ (Fig. 1D). Maximum earthquake size increases with convergence rate (Fig. 1E), simply because larger earthquakes are more probable at faster subduction zones (12). Subduction zones that have had $M_w \geq 8$ earthquakes have generally larger seismic consistency (Fig. 1F), a measure of the similarity of faulting during moderate-sized earthquakes occurring on the thrust fault (13), suggesting that they are smoother than segments that have not had great earthquakes.

Arguments for the possibility of great interplate thrust earthquakes at the CSZ are based on comparisons of the CSZ to other subduction zones with known seismic histories, on local geological observations of the effects of past earthquakes, and on modern strain rates in coastal regions. Largely on the basis of the gentle dip and young age of the subducting lithosphere, Cascadia has been compared to southern Chile, southwestern Japan, and Colombia, all of which produce great earthquakes (7) but none of which have significant forearc deformation (14). Concerning the age of the subducting plate, the coupling model considers only that young, warm, low-density lithosphere will resist sinking and increase coupling. Yet warm subducting lithosphere also heats the plate interface, decreasing the potential width (and area) of the part of the fault that is cool enough to produce earthquakes (15). Hence, thermal arguments predict an increase in earthquake size with the age of the subducting plate (although such a trend might be observable for only very young lithosphere because its temperature changes slowly after a few million years). A hint of this behavior can be seen in Fig. 1G. The data show that the largest earthquake (southern Chile) occurred where the subducting lithosphere has an average age of about 20 million years (16). (Because temperature gradients at the top of the lithosphere decrease as the square root of age, lithosphere with an age of 20 million years will supply roughly only 60% of the heat to the thrust fault as the lithosphere with an age of 6 million to 9 million years that subducts beneath Cascadia.) No global correlation is apparent between dip of the plate interface and earthquake size (Fig. 1H) (17).

Convergence at the 1400-km-long CSZ is 40 mm/year and 30° away from being perpendicular to the coast (18). Hence, motion of the Juan de Fuca plate relative to North America consists of 35 mm/year perpendicular to the margin and 19 mm/year right-lateral shear parallel to it. There have been no known thrust earthquakes at the CSZ to compare it to the global slip pattern of Fig. 1. However, recent marine geophysical surveys

show that the CSZ forearc between 43°N and 48°N deforms rapidly. Nine major west-northwest-trending, left-lateral, strike-slip faults have been mapped off the coasts of Oregon and Washington with SeaMARC-1A sidescan sonar and seismic reflection (2, 3) (Fig. 2). Five have slip rates, determined from offsets of submarine channels and dated sediment isopachs, of 5.5 to 8.5 mm/year. If the four faults for which slip rates could not be estimated have a slip rate of 5.5 mm/year (the smallest of the known rates), the arc-parallel (north-south) motion of the forearc reaches 17.4 mm/year, which nearly accounts for all arc-parallel plate motion. If the four unknown faults are not now slipping (even though two of them are among the clearest in the images), the net arc-parallel rate is 10.5 mm/year, still more than half the arc-parallel rate of plate motion. With additional deformation east of the coasts of Oregon and Washington (19), it is possible that all of the arc-parallel motion is absorbed by the upper plate. Clockwise rotations of Miocene-age Columbia River basalts inferred

from paleomagnetic declinations suggest that a large fraction of the transverse component of plate motion has been taken up by shear in the upper plate within 300 km of the plate boundary since 12 million to 15 million years ago (20).

In Fig. 1 we use the range of Cascadia forearc arc-parallel motion rates (10.5 to 17.4 mm/year), the plate convergence vector, and the maximum sizes of thrust earthquakes at other subduction zones to estimate the expected maximum size of subduction-zone earthquakes at Cascadia (the shaded areas show the ranges for Cascadia). Forearcs that have had earthquakes of $M_w > 8$ in this century show arc-parallel deformation rates generally below that of Cascadia (Fig. 1, A to D). The main exception is from the 1957 Aleutian earthquake (Fig. 1, B and C; $M_w = 9.0$), whose forearc shows a slip rate (Fig. 1B) larger than Cascadia and within the Cascadia range when the forearc slip rate is normalized by the full plate convergence rate (Fig. 1C). However, the arc-parallel component of plate motion near the 1957 Aleutian event is 2.5 times its value at Cascadia. We suggest that the best measure of forearc rigidity is the ratio V_f/V_p (the observed arc-parallel slip rate normalized by its maximum possible value), which indicates how fast the forearc deforms relative to the shearing rate at its base. This ratio provides a rough estimate of the relative importance of the forearc's anelastic and elastic responses to shearing. The low V_f/V_p values at forearcs with $M_w > 8$ earthquakes (Fig. 1D) suggests that the Cascadia forearc deforms more rapidly relative to the transverse component of plate motion than forearcs with $M_w > 8$ earthquakes. A forearc that shears so readily probably does not store the large elastic strains necessary for a great earthquake. The Marianas arc, often cited as the type example of a decoupled subduction zone, also has a large V_f/V_p value of ≈ 0.8 (14). The age and dip angle of the subducting plate do not render Cascadia any more likely than other subduction zones to have great thrust earthquakes (Fig. 1, G and H).

Observations of on-land deformation (21) and inferred temperatures of the thrust surface (15) suggest that the seismogenic part of the plate contact at the CSZ is narrow and does not extend as far landward as the coast. The plates are possibly now locked only below the offshore forearc that deforms rapidly. Nevertheless, a great earthquake could occur if the slip propagated a great distance along strike. Cross-forearc faults may act as barriers to this motion, and the CSZ has an abundance of active forearc faults. Transverse structural features are observed at other forearcs, such as the Aleutian and Nankai, that sometimes, but sometimes do not, act as barriers to propagating slip (22).

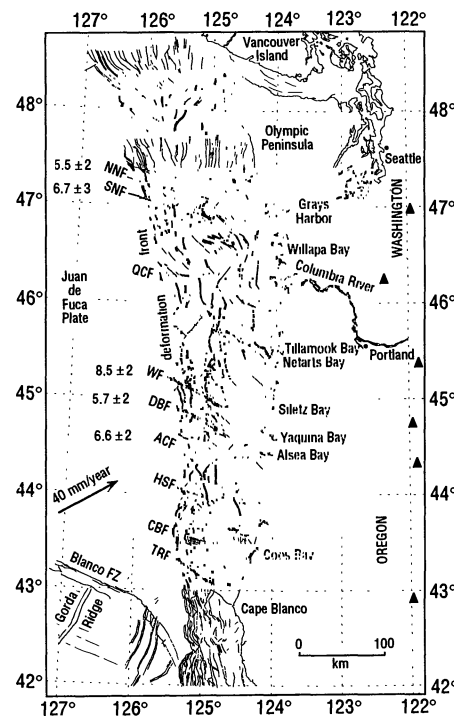


Fig. 2. Map of Quaternary and Pliocene structures of the Oregon and Washington continental margin (3). Slip rates for five faults are given in millimeters per year. The arrow shows the motion of the Juan de Fuca plate relative to North America, and triangles show locations of active Cascadia volcanoes. Abbreviations for west-northwest-trending left-lateral strike-slip faults, from north to south, are as follows: NNF, North Nitinat fault; SNF, South Nitinat fault; QCF, Quinalt Canyon fault; WF, We-coma fault; DBF, Daisy Bank fault; ACF, Alvin Canyon fault; HSF, Heceta South fault; CBF, Coos Basin fault; TRF, Thompson Ridge fault; and FZ, fault zone.

Evidence for repeated rapid deformation and shaking of the Oregon and Washington coastal areas has been used to infer a cycle of uplift and subsidence attributed to great subduction earthquakes (23). However, it is unknown what magnitude earthquake or rupture length is required to produce such effects at the coast. Holocene subsidence events in the coastal bays of Oregon and Washington and other upper-plate deformation may be caused by $M_w \approx 7.5$ or smaller (24) earthquakes within the forearc or $M_w \approx 8$ events on the plate interface, rather than by great (that is, $M_w \approx 9$) subduction events.

Cycles of great earthquakes at Pacific subduction zones are characterized by temporal regularity but irregularity in the sizes of earthquakes (25). A cycle often comprises several smaller events, instead of a single large one, occurring close together in time near the end of the cycle; multiple, similarly sized earthquakes typically cluster within 20% of the recurrence time (25). If the CSZ is characterized by a single $M_w > 9$ thrust earthquake every 600 years (the estimated repeat time for the sudden deformation and shaking events), it would indeed behave quite differently from known subduction zones. A sequence of several large events ($M_w \approx 8$ or smaller), each of which ruptures segments 100 to 200 km long, is more consistent with observations at other subduction zones. Such Cascadia events could span a period of 120 years (that is, 20% of the repeat time) and still satisfy geologic observations within uncertainties in the dates of the subsidence events and triggered turbidity currents (23). Several $M_w \approx 8$ or smaller earthquakes spread over a few decades pose a considerably smaller hazard to inhabited regions than a single event of $M_w \approx 9.5$ that ruptures the entire plate boundary (1).

Some modern forearcs show considerable vertical motion in addition to arc-parallel motion. The central Aleutian forearc moves relative to its backarc region at tens of millimeters per year (26), resulting in the formation of new basins within the forearc. Uplift rates of marine terraces near subduction zones are largely independent of the subduction stress regime (27) and do not correlate with maximum earthquake size (Fig. 11; any possible correlation is clearly negative). Large, upper-plate earthquakes are common; for example, of the $M_w > 7$ earthquakes in this century in Sumatra, which has a tectonic setting similar to that of Cascadia, at least half were upper-plate events. Upper-plate earthquakes may exhibit a deformation pattern that is in practice indistinguishable from that of the main thrust fault. Permanent aseismic deformation in the upper plate at Cascadia is suggested by the association of buried marshes with mapped upper-plate faults and folds (2, 3, 28). The complex

distribution of modern uplift rates of the Washington and Oregon coasts can be accounted for by permanent deformation of the upper plate (29), deformation of the upper plate associated with aseismic subduction of sea-floor topography, or simply the elastic response of a structurally heterogeneous upper plate, and not necessarily by the buildup of elastic strain preceding a great earthquake.

We conclude that the recent discovery of several upper-plate faults cutting the Cascadia forearc along with the global tendency of rapidly deforming forearcs to be void of great ($M_w > 8$) earthquakes requires a reevaluation of the seismic hazards in the Pacific Northwest. Many observations used to infer a history of great subduction earthquakes and interpretations of modern strain accumulation are based on assumptions of an elastic upper plate. The conclusions of such work should be reexamined in light of clear evidence for an anelastic, rapidly deforming upper plate at Cascadia. We suggest that anelastic deformation of the upper plate and smaller, upper-plate earthquakes can account for most observations and that a great subduction earthquake at Cascadia is not inevitable.

REFERENCES AND NOTES

1. Moment magnitude is defined as $M_w = 2/3 \log M_0 - 10.7$, where M_0 is the seismic moment in dyne-centimeters [T. Hanks and H. Kanamori, *J. Geophys. Res.* **84**, 2348 (1979)]. M_0 is the product of faulting area, average slip, and rigidity of the rocks; M_0 and the amplitude of ground motion increase by a factor of 32 when M_w increases by 1 unit.
2. C. Goldfinger *et al.*, *Geology* **20**, 141 (1992); B. Applegate *et al.*, *Tectonics* **11**, 465 (1992).
3. C. Goldfinger, thesis, Oregon State University (1994).
4. Hazards posed by onshore faults are not well known, but some structures are possibly seismogenic [R. C. Bucknam, E. Hemphill-Haley, E. B. Leopold, *Science* **258**, 1611 (1992)]. Earthquakes of magnitude 7.1 in 1949 and 6.5 in 1965 occurred in the slab beneath Puget Sound.
5. H. Kanamori, in *Island Arcs, Deep Sea Trenches, and Backarc Basins*, M. Talwani and W. C. Pitman III, Eds. (Maurice Ewing Series 1, American Geophysical Union, Washington, DC, 1977), p. 163.
6. L. Ruff and H. Kanamori, *Phys. Earth Planet. Inter.* **23**, 240 (1980); *Tectonophysics* **99**, 99 (1983); S. Uyeda and H. Kanamori, *J. Geophys. Res.* **84**, 1049 (1979); L. Ruff, *Pure Appl. Geophys.* **129**, 270 (1989).
7. T. H. Heaton and H. Kanamori, *Bull. Seismol. Soc. Am.* **74**, 933 (1984); T. H. Heaton and S. H. Hartzell, *Science* **236**, 162 (1987); G. C. Rogers, *Can. J. Earth Sci.* **25**, 844 (1988).
8. If the forearc of the upper plate is rigid, then subduction earthquakes will slip in the direction of the relative plate motion. If the forearc moves relative to the backarc region of the upper plate, then the slip shows the relative motion between the subducting plate and the forearc. Simple geometry relates the expected slip rate and direction, the angle through which the slip direction is deflected, and the rate of forearc motion in the arc-parallel direction. R. Jarrard, *Rev. Geophys.* **24**, 217 (1986); M. Beck, *Phys. Earth Planet. Inter.* **68**, 1 (1991); R. McCaffrey, *J. Geophys. Res.* **97**, 8905 (1992).
9. Moment magnitudes for earthquakes before 1977 are from the J. Pacheco and L. Sykes [Bull. Seismol. Soc. Am. **82**, 1306 (1992)] (PS) catalog and for earthquakes from 1977 to September 1993 are from the Harvard centroid-moment tensor (CMT) catalog [A. Dzierwinski, T.-A. Chou, J. H. Woodhouse, *J. Geophys. Res.* **86**, 2325 (1981)]. We selected all thrust earthquakes that occurred near South America, Middle America, Antilles, Aleutian, Kuriles, Japan, Solomon, New Hebrides, Tonga, Izu-Bonin-Mariana, Ryukyu, Philippine, Sandwich, and Java trenches. Lengths of individual trenches should not limit earthquake size because all are more than 1000 km long, except Japan, which is 650 km long. The largest known earthquake, the 1960 Chile event of $M_w = 9.5$, had a rupture length of 1000 km (25). Of the 96 events selected from the PS catalog, 25 do not have estimates of seismic moment independent of the surface-wave magnitude M_s but these are below $M_s = 8$ and should not be affected by saturation of the M_s scale that occurs above $M_s \approx 8.1$ [R. Geller, *Bull. Seismol. Soc. Am.* **66**, 1501 (1976)]; for these we let $M_w = M_s$. Whether the instrumental earthquake record for this century is representative of longer term earthquake patterns is not known. Inferences about Cascadia subduction earthquake potential, including ours and earlier ones that use the short historical record, are subject to this uncertainty.
10. Heterogeneity of the fault surface may impose barriers to expansion of the fault rupture and limit earthquake size [T. Lay, H. Kanamori, L. Ruff, *Earthquake Predict. Res.* **1**, 3 (1982)].
11. We use the term anelastic in the sense that the strain in the forearc is time-dependent and not recoverable. Such strain may occur during earthquakes within the upper plate; an earthquake itself results from an elastic process, but the accumulated slip over many earthquakes is anelastic.
12. R. McCaffrey, *Geophys. Res. Lett.* **21**, 2327 (1994).
13. Seismic consistency C_s of a group of earthquakes is defined by C. Frohlich and K. D. Apperson [*Tectonics* **11**, 279 (1992)] as the scalar moment of the sum of the moment tensors divided by the sum of their scalar moments. When all earthquake mechanisms are identical, $C_s = 1$. Moment tensors are taken from the CMT catalog (1977 through 1993).
14. R. McCaffrey, *J. Geophys. Res.* **98**, 11953 (1993); *Pure Appl. Geophys.* **142**, 173 (1994).
15. R. Hyndman and K. Wang, *J. Geophys. Res.* **98**, 2039 (1993).
16. The 1960 Chile event ruptured the plate boundary along the region where subducting lithosphere ranges in age from 0 to 35 million years. However, it began at the northern end of the rupture area where the oldest lithosphere is subducting.
17. J. Pacheco, L. R. Sykes, C. H. Scholz, *J. Geophys. Res.* **98**, 14133 (1993).
18. The Juan de Fuca-North America relative motion is estimated from the Juan de Fuca-Pacific pole and Pacific-North America pole [C. DeMets, R. G. Gordon, D. F. Argus, S. Stein, *Geophys. J. Int.* **101**, 425 (1990); D. Wilson, *J. Geophys. Res.* **93**, 11863 (1988)].
19. S. K. Pezzopane and R. J. Weldon, *Eos* **73**, 527 (1992); W. C. Grant, C. S. Weaver, J. E. Zollweg, *Bull. Seismol. Soc. Am.* **74**, 1289 (1984).
20. M. Beck, *Am. J. Sci.* **276**, 694 (1976); P. England and R. Wells, *Geology* **19**, 978 (1991); R. Wells and R. Coe, *J. Geophys. Res.* **90**, 1925 (1985).
21. H. Melosh and K. Wang, *Eos* **73**, 527 (1992); J. C. Savage, M. Lisowski, W. H. Prescott, *J. Geophys. Res.* **96**, 14493 (1991).
22. H. F. Ryan and D. W. Scholl [*J. Geophys. Res.* **98**, 22135 (1993)] suggested that rotating forearc blocks control the seismic character of the Aleutian subduction zone, including the locations and rupture extents of great earthquakes. R. Yeats, K. E. Sieh, and C. R. Allen [*Geology of Earthquakes* (Oxford Univ. Press, Oxford), in press] present a summary of the relation of great earthquakes to cross-forearc structural features.
23. B. F. Atwater, *Science* **236**, 942 (1987); J. Adams, *Tectonics* **3**, 449 (1984); B. Atwater and D. Yamaguchi, *Geology* **19**, 706 (1991); J. Adams, *Tectonics* **9**, 569 (1990).
24. The cross-forearc strike-slip faults are about 100 km long from the trench to the coast and extend down to the subducting plate, which dips from the sea floor at the trench to a depth of about 20 km beneath the coast [A. M. Trehu *et al.*, *Science* **266**, 237 (1994)]. The contact area offshore is then approximately 1000

- km². The rigidity (2×10^{10} N/m²) is the density (2600 kg/m³) multiplied by the square of the shear wave speed (2800 m/s), which is assumed to be the average compressional wave speed in the offshore forearc rocks (5000 m/s) divided by 1.75. If the slip is 1 m, the seismic moment (M) is 2×10^{19} N-m, for $M_w = 6.8$. For a large value of slip (5 m) on the same fault, $M_w = 7.3$. The regression formula of D. Wells and K. Coppersmith [*Bull. Seismol. Soc. Am.* **84**, 974 (1994)] relates magnitude to fault length for California strike-slip earthquakes; $M = 5.16 + 1.12 \log(\text{length})$. After correction for differences in shapes of the fault areas (Cascadia forearc strike-slip faults are triangular instead of rectangular in cross section), this formula indicates a magnitude of 7.2 for a length of 100 km.
25. W. Thatcher, *J. Geophys. Res.* **95**, 2609 (1990).
 26. G. Ekström and R. Engdahl, *ibid.* **94**, 15499 (1989); E. Geist, J. R. Childs, D. W. Scholl, *Tectonics* **7**, 327 (1988).
 27. R. Jarrard [*Rev. Geophys.* **24**, 217 (1986)] defined several strain classes for subduction zones, ranging from strongly compressional (active backarc thrusting) to extensional (active backarc spreading). D. Muhs *et al.* [*J. Geophys. Res.* **95**, 6685 (1990)] showed that forearc uplift rates do not correlate with these strain classes.
 28. G. McInnelly and H. Kelsey, *J. Geophys. Res.* **95**, 6699 (1990).
 29. J. C. Savage and M. Lisowski, *Science* **252**, 101 (1991); C. Mitchell, P. Vincent, R. J. Weldon, M. A. Richards, *J. Geophys. Res.* **99**, 12257 (1994). H. Kelsey, D. C. Engebretson, C. E. Mitchell, and R. L. Ticknor (*ibid.*, p. 12245) showed that the along-strike variations in uplift rate mapped by Mitchell *et al.* correlate with topography and may be due to permanent uplift rather than seismic strain accumulation.
 30. R. D. Mueller, W. R. Roest, J. Y. Royer, L. M. Gahagan, J. G. Sclater, *SIO Reference Series* **93-30** (1993).
 31. We thank V. Kulm, R. Yeats, A. Trehu, and J. Nabelek for discussions and R. Lillie and A. Nelson for reviews of an early manuscript. Supported by National Science Foundation grants OCE-9216880 [Oregon State University (OSU)], EAR-9105050 [Rensselaer Polytechnic Institute (RPI)], and EAR-9406917 (RPI), U.S. Geological Survey National Earthquake Hazards Reduction Program under awards 1434-93-G-2319 and 1434-93-G-2489 (OSU), and the National Oceanic and Atmospheric Administration Undersea Research Program, West Coast National Undersea Research Center at the University of Alaska, grants UAF-92-0061 and UAF-93-0035 (OSU).

13 September 1994; accepted 14 December 1994

Galaxies, Human Eyes, and Artificial Neural Networks

O. Lahav, A. Naim, R. J. Buta, H. G. Corwin, G. de Vaucouleurs, A. Dressler, J. P. Huchra, S. van den Bergh, S. Raychaudhury, L. Sodré Jr., M. C. Storrie-Lombardi

The quantitative morphological classification of galaxies is important for understanding the origin of type frequency and correlations with environment. However, galaxy morphological classification is still mainly done visually by dedicated individuals, in the spirit of Hubble's original scheme and its modifications. The rapid increase in data on galaxy images at low and high redshift calls for a re-examination of the classification schemes and for automatic methods. Here are shown results from a systematic comparison of the dispersion among human experts classifying a uniformly selected sample of more than 800 digitized galaxy images. These galaxy images were then classified by six of the authors independently. The human classifications are compared with each other and with an automatic classification by an artificial neural network, which replicates the classification by a human expert to the same degree of agreement as that between two human experts.

Hubble (1) suggested a classification scheme for galaxies that consists of one sequence starting from elliptical galaxies

O. Lahav, A. Naim, M. C. Storrie-Lombardi, Institute of Astronomy, Madingley Road, Cambridge CB3 0HA, UK.

R. J. Buta, Department of Physics and Astronomy, University of Alabama, Tuscaloosa, AL 35487-0324, USA.
H. G. Corwin, California Institute of Technology, IPAC M/S 100, Pasadena, CA 91125, USA.

G. de Vaucouleurs, Department of Astronomy, RLM 15.308, University of Texas, Austin, TX 78712-1083, USA.

A. Dressler, Carnegie Observatories, 813 Santa Barbara Street, Pasadena, CA 91101-1292, USA.

J. P. Huchra and S. Raychaudhury, Harvard-Smithsonian Center for Astrophysics, 60 Garden Street, Cambridge, MA 02138, USA.

S. van den Bergh, Dominion Astrophysical Observatory, 5071 West Saanich Road, Victoria, British Columbia, V8X 4M6, Canada.

L. Sodré Jr., Instituto Astronômico e Geofísico da Universidade de São Paulo, CP9638, 01065, São Paulo, Brazil.

(E), through lenticular galaxies (S0), to spiral galaxies (S) and a parallel branch of spirals with a barred component, which yields the so-called "tuning fork" Hubble diagram. This scheme has been extended by astronomers over the years (2-5) to incorporate features such as the strength of the spiral arms, yielding multidimensional classifications (3, 5). It is remarkable that these somewhat subjective classification labels for galaxies (as seen projected on the sky) correlate well with physical properties such as color, dynamical properties (for example, rotation curves and stellar velocity dispersions), and the mass of neutral hydrogen (6). However, one would like eventually to devise a scheme of classification that can be related to the physical processes of galaxy formation. Although there have been in

recent years significant advances in observational techniques (for example, in the telescopes, detectors, and reduction algorithms) and in theoretical modelling (for example, N -body and hydrodynamics simulations), galaxy classification remains a subjective area.

Quantifying galaxy morphology is important for various reasons. First, it provides important clues to the origin of galaxies and their formation processes. For example, elliptical and lenticular galaxies make up only ~20% of the galaxies, and there is a striking density-morphology relation (1, 7), indicating that elliptical galaxies mainly reside in high-density regions. Understanding the origin of the type frequency and the density-morphology relation is of fundamental importance. However, quantification of these properties requires reliable classification schemes. Second, galaxies can also be used to, for example, measure redshift-independent distances by methods such as the luminosity-rotation velocity relation for spirals (8) and the diameter-velocity dispersion relation for ellipticals (9). Any observational program requires an a priori list of target objects for photometric or spectrographic measurements. Therefore, galaxy classification is important for the practical goal of producing large catalogs for statistical and observational programs and for establishing some underlying physics (in analogy with the Hertzsprung-Russell diagram for stars). Moreover, understanding the morphology of galaxies at low redshift is crucial for any meaningful comparison with galaxy images obtained with the Hubble Space Telescope at higher redshift ($z \approx 0.4$). Most of our current knowledge of galaxy morphology is based on the pioneering work of several dedicated observers, who have classified and cataloged thousands of galaxies (2, 10, 11). However, facilities such as the Cambridge Automated Plate Measuring (APM) machine and the Sloan digital sky survey yield millions of galaxies. Classifying very large data sets is obviously beyond the capability of a single person. Therefore, the galaxy classification problem calls for new approaches (12-16).

As a first step toward finding an automated method of galaxy classification, we compiled a well-defined sample of galaxy images. The galaxies were chosen from the APM Equatorial Catalogue of galaxies (17). This sample was compiled from IIIaJ (broad blue-green band) plates taken with the United Kingdom's Schmidt telescope at Siding Spring, Australia; the sample covers most of the sky between declinations -17.5° and 2.5° at galactic latitudes $b \geq 20^\circ$. We chose a subsample of galaxies with major diameter (at an isophotal level of 24.5 magnitudes per square arc sec) $D \geq 1.2$ arc min on 75 plates, after eliminating gal-